Spectrum Sensing Applications of FWM-based Optical Cyclostationary Processor

Jerrod Langston[1,2], Richard DeSalvo[2], Stephen E. Ralph[1]
[1]*School of Electrical and Computer Engineering, Georgia Institute of Technology, Atlanta, GA, USA*
[2]*L3Harris, Melbourne, FL, USA*
Email: stephen.ralph@ece.gatech.edu

Abstract: We demonstrate a large instantaneous bandwidth optical cyclostationary processor that computes the spectral correlation function. Post-processing of experimentally measured SCFs is applied for waveform characterization, specifically baud rate and pulse-shaping roll-off estimation of QAM signals.

1. Introduction

Cyclostationary (CS) analysis is an important tool for spectrum sensing that enables the observation and classification of communication waveforms in crowded spectral domains. For example, CS techniques can discriminate between waveforms with overlapping spectra, assuming unique baud rates or carrier frequencies. Conventional CS processors (CSPs) apply the required operations completely in the digital domain, which directly limits the potential instantaneous bandwidth and introduces processing latency. With the increase in carrier frequencies and signal bandwidths, CSPs must correspondingly increase in capability: optical signal processing is a technology that can be utilized to address these needs [1].

We describe a large instantaneous bandwidth, optical CSP that enables evaluation of the spectral correlation function (SCF) for wide-band signals. The OCSP reduces the computation load of digital signal processors using the FFT accumulation methods (FAM) [2], by using optical delays for high-resolution frequency shifting and nonlinear optical signal processing for conjugate multiplication. The experimentally evaluated SCF is shown for some sample, wide-bandwidth waveforms. Finally, additional DSP is applied to the experimentally measured SCF for use in spectrum sensing applications.

2. Theory

2.1 CSP Theory

The purpose of the architecture presented is to evaluate the SCF which can be approximated as the cyclic periodogram [3]:

$$\mathcal{S}_{x,T}^{\alpha}(t,f) = \frac{1}{T} X_T\left(t, f + \frac{\alpha}{2}\right) X_T^*\left(t, f - \frac{\alpha}{2}\right) \tag{1}$$

where X_T is the Fourier transform of the signal $x(t)$ at time t and α is the cyclic frequency. This multi-dimensional function provides information about detected signals not easily gleaned from the power spectral density (PSD), especially when overlapping signals are present. The FAM involves averaging multiple cyclic periodograms, computed using the listed operations. Averaging is used to smooth the evaluated cyclic spectrums for increased spectrum estimation accuracy.

2.2 Communication Waveform Signatures

Conventional, linearly modulated communication waveforms, such as *M*-PSK or *M*-QAM, exhibit second-order cyclostationarity thus exhibit signatures in the SCF at the cyclic frequency corresponding to the baud rate. Baud rate estimation can then be complete by estimating the cyclic frequency that yields a non-zero magnitude (other than zero). Not only this, but the shape of the cyclic spectrum is unique for different pulse shapes. In fact, root-raised cosine (RRC) shaping is commonly used in optical and wireless links and its analytical cyclic spectrum can be demonstrated to be:

$$\mathcal{S}_{\text{RRC}}^{\alpha=f_b}(\tilde{f}) = \begin{cases} \cos(\pi\tilde{f}/\beta) & |\tilde{f}| < \beta/2 \\ 0 & \text{else} \end{cases} \tag{2}$$

where f_b is the baud rate, β is the roll-off factor, and $\tilde{f} = f/f_b$ is the normalized frequency. Note the simple shape description compared to the PSD, and that as the roll-off factor approaches zero the cyclic spectrum approximates a delta function. The cyclic spectrum of raised cosine shaping can similarly be derived and is the square of the Eq. 2.

3. Experimental Setup

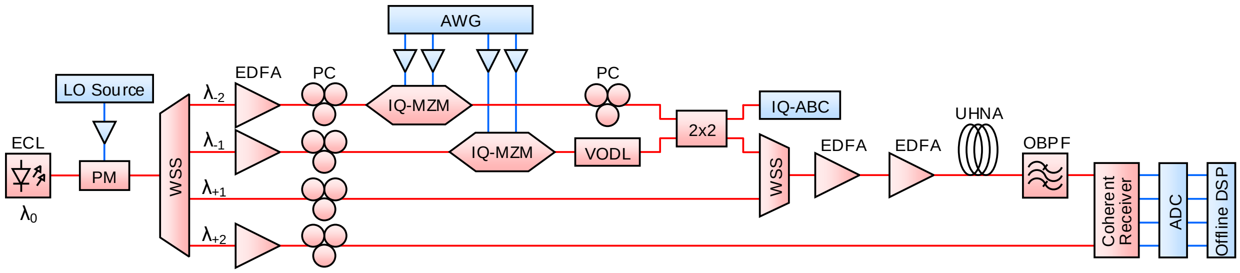

Fig. 1: Block diagram of OCSP

3.1 Hardware Setup

The architecture of the OCSP used to evaluate the SCF is shown in Fig. 1. A low-linewidth, 1550-nm laser (labelled λ_0) is phase modulated (PM) to generate an optical comb. A wavelength selective switch (WSS) demultiplexes the optical comb line such that first- and second-harmonic, upper- and lower-sidebands are passed to separate optical branches. The top two branches correspond the two signal paths of the OCSP, wherein the lower sidebands (λ_{-2} and λ_{-1}) are separately modulated by the complex Fourier coefficients of the signal in question, that is, the frequency-to-time mapping of the signal. A variable optical delay line (VODL) enables fine tuning of the timing offset between the two paths (corresponding to a cyclic frequency offset). Polarization controllers are utilized throughout the link to ensure correct alignment for optimal modulation and optical mixing.

The signal paths are coupled together, with a tap used for automatic bias control (ABC) of the IQ-MZMs, and multiplexed with the first upper-sideband of the optical comb (λ_{+1}) using a second WSS. Though a coupler could provide the necessary multiplexing, a second WSS provides further suppression of out-of-band optical comb lines not suppressed completely by the first WSS as well as independent gain control of the sidebands. The combined signals and optical pump are amplified and fed through 16-m of ultra-high numerical aperture (UHNA) fiber. The high-power optical pump and highly nonlinear fiber facilitate efficient four-wave mixing (FWM). Various FWM terms are generated, with the term of interest located at the second-harmonic upper-sideband of the optical comb. An optical bandpass filter (OBPF) selects the FWM term of interest, which is proportional to the conjugate multiplication of the signal amplitudes, that is, $A_{-1}A^*_{-2}A_{+1}$. The filtered term is captured by a coherent receiver with the optical LO being the second-harmonic upper-sideband of the optical comb, thus the electrical outputs, which are subsequently digitized, have no frequency offset and minimal phase fluctuations.

3.2 OCSP DSP

To properly evaluate the SCF, the OCSP requires transmitter- and receiver-side DSP. The Fourier coefficients generated by the arbitrary waveform generator (AWG) are structured within frames. The beginning of the frames contain known, but independent timing recovery headers, such that, at the receiver, the capture waveform can be correlated with the conjugate multiplication of the transmitted headers for synchronization. Also included in the frames are pilot tones placed periodically so that phase fluctuations with time can be tracked. The Fourier coefficients themselves are structured such that within different sections of the frame, there are different timing offsets between the two input signal coefficients corresponding to different cyclic frequencies. By sweeping over all numerous cyclic frequencies and capturing and averaging the cyclic spectrums, the SCF can be generated.

3. Experimental Results

To first demonstrate functionality of the OCSP, the SCF of various waveforms were computed to investigate wide-bandwidth signals, multiple closely-space signals, and low-bandwidth signals (much lower than the OCSP bandwidth). One such SCF is that of 15-Gbd 16QAM, which is shown in Fig. 2a, and was created from averaging 200 SCFs. Fig. 2b displays the improvement in spectrum estimation of the PSD when averaging different amounts. Note, this does not yield a higher SNR of the detected signal, but a more accurate estimation of the PSD. Similarly, Fig. 2c displays the cyclic spectrum evaluated at 15-Gbd with different amounts of averaging. As expected, the cyclic spectrum estimation improves with averaging. Though not shown, the phase responses similarly exhibit similar good estimation accuracy.

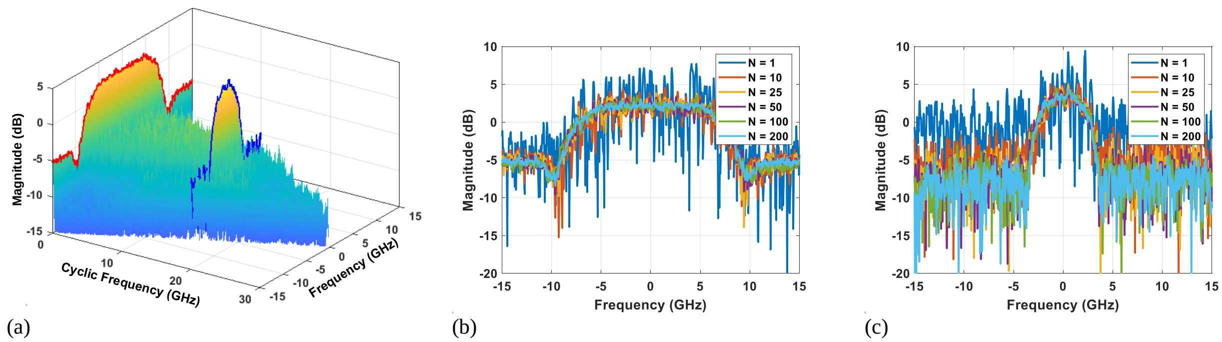

Fig. 2: Experimentally measured (a) SCF, (b), PSD and (c) cyclic spectrum of 15-Gbd 16QAM

With the experimentally measured SCF a few steps can be taken to characterize the waveforms in question. The first step is to estimate the baud rate. By averaging the SCF with respect to frequency, clear peaks can be seen corresponding to zero cyclic frequency and the baud rate cyclic frequency (Fig. 3a). By completing a peak search across cyclic frequency, ignoring zero, the baud rate is easily estimated. Note, this method of baud rate requires fine cyclic frequency resolution so that true cyclic frequencies are not neglected.

The second step taken is to estimate the pulse shaping roll-off from the cyclic spectrum at the estimated baud rate of the waveform in question. Because an analytical expression for the cyclic spectrum due to RRC pulse shaping is known with low-complexity, a nonlinear regression algorithm, in this case the Levenberg-Marquardt algorithm [], is used to estimate the parameter β as well as the cyclic spectrum amplitude. Fig. 3b. shows the measured cyclic spectrum with overlapping RRC regression. In this example, the estimated roll-off was 0.492 compared to the actual roll-off of 0.5, corresponding to an estimation error ~1%. This classification accuracy is extremely high: about an order of magnitude more accurate than required for reasonable matched filtering.

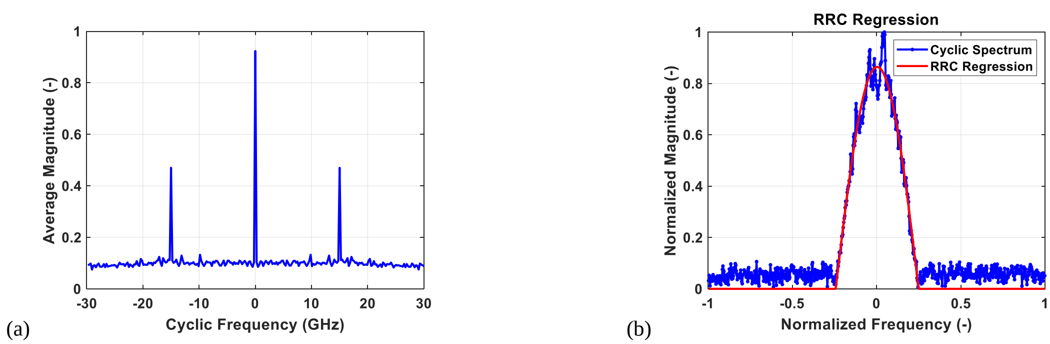

Fig. 3: Experimentally captured (a) average SCF for baud rate estimation and (b) cyclic spectrum of 15-Gbd 16QAM with RRC pulse shaping

4. Conclusions

We experimentally demonstrated accurate computation of the SCF of wideband signals by an OCSP, utilizing some optical signal processing techniques to reduce the digital computational load. Signal analysis was subsequently applied to the SCFs, to demonstrate the practicality of the OCSP for waveform characterization and interrogation.

5. References

[1] D. J. Esman et al., "Comb-Assisted Cyclostationary Analysis of Wideband RF Signals," *J. Lightw. Technol.*, vol. 35, no. 17, pp. 3705-3712, Sept. 2017.

[2] R. S. Roberts et al., "Computationally Efficient Algorithms for Cyclic Spectral Analysis," in *IEEE SP Magazine*, vol. 8, no. 2, pp. 38-49, Apr. 1991.

[3] W. A. Gardner, *Statistical Spectral Analysis: A Nonprobabilistic Theory*, (Prentice Hall, 1988).